

Structural, Optical and Antimicrobial Properties of Carbohydrate-Capped Cadmium Sulfide Nanoparticles

Subhav Adhikari¹, Kshama Parajuli^{1*}, Guna B. Karki¹,
Shankar P. Khatiwada¹, Rameshwar Adhikari^{1,2*}

¹Central Department of Chemistry, Tribhuvan University, Kirtipur, Kathmandu 44618, Nepal

²Research Centre for Applied Science and Technology (RECAST), Tribhuvan University, Kirtipur, Kathmandu 44600, Nepal

*Authors for correspondence (kshamaparajuli@yahoo.com, nepalpolymer@yahoo.com)

Submitted: 28 Nov 2022, Revised: 31 Dec 2022, Accepted: 7 Jan 2023

Abstract

Cadmium sulfide nanoparticles (CdSNPs) were prepared through the chemical precipitation process where sweet potato starch and glucose functioned as capping agents. Ultraviolet-Visible (UV-Vis) spectroscopy, Fourier Transform Infrared (FTIR) spectroscopy and X-ray diffraction (XRD) techniques were applied for the analysis of prepared CdSNPs. The absorption peaks in the UV-Vis spectroscopy towards the lower wavelength region compared to the bulk CdS (512 nm) indicated the formation of CdS particles in the nanometer scale range. FTIR spectroscopy showed the characteristic absorption peaks of the CdSNPs along with the functional groups present in starch and glucose, suggesting the possible interaction between CdSNPs and capping agents. The XRD revealed crystallographic information such as the average crystallite size and shape of CdSNPs. Using the Scherrer equation, the average crystallite size of CdSNPs was determined to be 11.48 nm and 16.03 nm for starch-capped and glucose-capped CdSNPs (CdS-St and CdS-Gl) respectively. Antibacterial and antifungal activities of the prepared CdSNPs were found to be highly efficient for various pathogenic bacteria and fungi. Hence in the present study, the new synthetic route of CdSNPs was applied, and antimicrobial activities were performed

Keywords: *Chemical precipitation, Cadmium sulfide nanoparticles, FTIR spectroscopy, X-ray diffraction, UV-Visible spectroscopy*

1. Introduction

In recent years, nanoparticles (NPs), having a diameter between 1-100 nm have gained much research concern because of their different attractive optoelectronic, electrical, and antimicrobial properties [1-4]. It has been indeed established that, on decreasing the size of materials to the range of nanometers, their physical, chemical, and biological properties drastically change owing to the large surface area, the existence of electrostatic force and resulting quantum size effects etc. [5]. As a result, the NPs are used these days in advanced applications including energy generation,

environmental remediation, food industries and medicine [6-8].

Preparation and characterization of some important semiconducting nanomaterials such as CdO, ZnS, ZnO, CdS, CdSe and CdTe NPs are comprehensively reported in the literature [9, 10]. In this regard, the CdS NPs are one of the most widely studied binary chalcogenides amongst II-IV groups, owing to their wide band gap energy of 2.43 eV in the bulk state and resulting in excellent photosensitivity [11, 12]. Different chemical methods comprising

microemulsions, condensation and hydrothermal techniques, the use of ultrasonic radiation [13-17] as well as biological processes [18] are used in the preparation of CdSNPs. However, the use of these methods was limited because of low yields, excessive cost, tedious synthetic procedures, and the use of various toxic chemicals. In those methods, various chemicals such as dimethylformamide, thioglycerol, thiourea, sodium dodecyl sulphate, diethylenetriamine, cetyltrimethylammonium bromide, 3-mercaptopropionic acid and thiophenol have been used as capping agents which might cause health and environmental issues [13-19].

Cadmium sulfide nanoparticles (CdSNPs) find wide applications in photocatalysis, biosensors and targeted drug delivery [20,21], one of their vital applications being their use as novel antibacterial and antifungal agents [22-25]. The electrostatic interaction between positively charged cadmium ions and negatively charged proteins on the cell wall of bacteria might disrupt the latter due to the formation of reactive oxygen species [26, 59] which makes the CdSNPs an effective antibacterial agent. Similarly, the antifungal activity of the CdSNPs has been studied by researchers [23, 24, 26-29]. It has been found that when fungi are exposed to NPs for a prolonged period, they may form pits on their cell surfaces causing pores formation and apoptosis [27, 28].

This work aims to synthesize CdSNPs by using non-toxic, less hazardous, and eco-friendly green capping agents such as sweet potato starch (SPS) and glucose. The synthesis was carried out by a simple, less time-consuming, and economic chemical precipitation method [30]. The synthesized NPs were characterized by FTIR spectroscopy, UV-Vis spectroscopy and powder XRD. The synthetic route of CdSNPs was optimized and the antibacterial and antifungal properties of CdS NPs were also investigated against different microbial strains.

2. Material and methods

2.1 Materials

Cadmium nitrate ($\text{Cd}(\text{NO}_3)_2$), sulphuric acid (H_2SO_4), sodium hydroxide (NaOH), ethanol ($\text{C}_2\text{H}_5\text{OH}$) and

glucose were purchased from Fisher Scientific, India. Starch was extracted from sweet potatoes collected from the nearby area in Tribhuvan University, Kathmandu using standard procedure [31]. All solutions were prepared in distilled water. A Gram-positive bacterial strain viz. *Staphylococcus aureus* (ATCC 25923) and three Gram-negative species viz. *Escherichia coli* (ATCC 25922), *Salmonella typhi* and *Pseudomonas aeruginosa* (ATCC 27853) as well as four fungal strains viz. *Aspergillus niger*, *Aspergillus flavus*, *Trichoderma* and *Rhizopus* were used for antimicrobial tests.

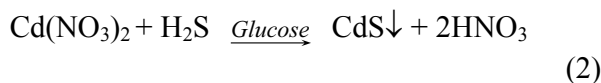
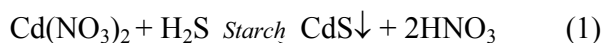
2.2 Preparation of solutions

Preparation of SPS solution: Fresh sweet potato rhizomes were taken from Kathmandu and cleaned with distilled water for the removal of all kinds of impurities. Then rhizomes were peeled off, sliced into small pieces, and air-dried. 50 g of the dry sweet potato slices were taken in a dry and clean kitchen blender and ground into a smooth slurry together with distilled water. The slurry was filtered through a finely fabricated cotton cloth to obtain starch suspension which was then settled for 12 h in a refrigerator maintained at 10°C. The supernatant liquid was removed followed by drying the collected sediment at 45°C for 7 h in a hot air oven to get the required SPS. Then, 7 g of thus obtained SPS was mixed with 100 mL of water and 10 mL of the SPS solution was used in the synthesis of CdSNPs.

Preparation of glucose solution: 1.8 g of purchased glucose was mixed in 100 mL of water and 10 mL of the glucose solution was used in the preparation of CdSNPs.

2.3 Synthesis of CdSNPs: Aqueous solutions of $\text{Cd}(\text{NO}_3)_2$ (100 mL, 0.1 mol L⁻¹) were prepared in two separate round bottom flasks. The above-prepared starch and glucose solutions were then added dropwise to the separate solutions containing $\text{Cd}(\text{NO}_3)_2$ followed by continuous passing of H_2S gas under constant stirring at 500 rpm. The pH level was maintained at 10 by drop-wise addition of ammonia solution. The colour of the solution gradually changed from light to dark yellow. Both mixtures were allowed

to constantly stir for 24 h for the completion of CdSNPs synthesis. The chemical reactions involved herein are given in equations (1) and (2).



The precipitate was washed several times with distilled water followed by ethanol. Finally, the resulting clear orange-yellow pellets of CdSNPs were obtained by evaporating the solvents at 23°C. Thus, synthesized samples of Starch (St) capped and Glucose (Gl) capped CdSNPs were denoted as CdS-St and CdS-Gl, respectively.

2.4 Characterization methods

Fourier-transform infrared (FTIR) spectroscopy was used in the identification of the infrared spectra of capping agents and synthesized NPs using an IR-Tracer-100 Spectrometer (Shimadzu, Japan) in the wavenumber range of 400–4000 cm⁻¹.

Ultraviolet-visible (UV-vis.) spectroscopy was performed using Chemito UV-Visible spectrophotometer for the analysis of the optical properties of synthesized NPs. The well-dispersed colloidal solution of CdSNPs was used and its absorbance was measured in the wavelength region of 450–750 nm.

X-ray diffraction (XRD) used was D-2 Phaser Advanced Diffractometer (Bruker, Germany), run at 30 kV and 10 mA with monochromatic Cu-K α radiation performed under ambient conditions over the 2 θ region of 20° to 80° at the rate of 2°/min. This method was used to determine the size and crystallography of the NPs. The crystallite size (D) was determined by using Scherrer's formula [32]:

$$D = \frac{0.9\lambda}{\beta \cos \theta} \quad (1)$$

where,

D = the mean size of the ordered (crystallite) domains (in nanometers)

λ = X-ray wavelength ($\lambda = 1.54046 \text{ \AA}$ for Cu-K α radiation)

β = full width at half maximum (FWHM) (in radian)

θ = Bragg's diffraction angle (in degrees)

2.5 Antimicrobial activity:

25 mg of CdSNPs was dissolved in 1 mL of dimethyl sulphonyloxide and screening, as well as evaluation of the antimicrobial activity, was performed [18]. For the antibacterial test, four bacterial species; *S. aureus*, *E. coli*, *S. typhi* and *P. aeruginosa* were cultured in Mueller Hinton Broth and 4 h after the culture, standard McFarland was matched. Then bacterial strains were swabbed, and wells were made on Mueller Hinton Agar (MHA) plate. 50 μL of the prepared CdSNPs (25 mg/mL) and positive control (Neomycin, 1 mg/mL) were loaded into the wells followed by incubation for a day at 37°C.

Similarly, for the antifungal tests, four fungal species; *A. niger*, *A. flavus*, *Trichoderma* and *Rhizopus* were cultured in Potato Dextrose Broth for 3 days at 28°C. These strains were swabbed, and then wells were made on the Potato Dextrose Agar plate. 50 μL of the prepared CdSNPs (25 mg/mL) and positive control (cycloheximide, 25 mg/mL) were loaded into the wells. It was subjected to incubation for 3 days at 28°C. The inhibitions in both above-mentioned tests were observed on the following day and zones of inhibition were measured.

3. Results and discussion

3.1 Structural characterization

Figure 1 depicts the FTIR plots of starch-capped and glucose-capped CdSNPs (CdS-St and CdS-Gl) powder. The broad absorption band around 3270 cm⁻¹ (i.e., 3280 cm⁻¹ for CdS-St and 3265 cm⁻¹ for CdS-Gl) is assigned to the O-H stretching mode of starch, glucose, and adsorbed water. Such an observation was also reported earlier for sweet potato and cassava starch [33] and bare CdS [34].

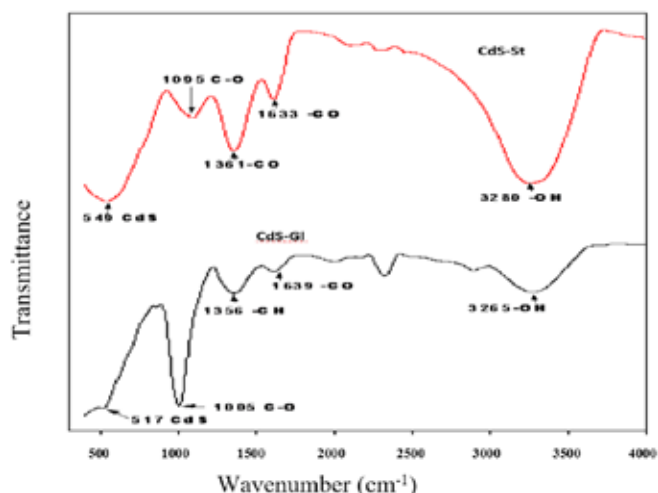


Figure 1. FTIR spectra of starch and glucose-capped CdSNPs (CdS-St and CdS-Gl) in the range of 400-4000 cm^{-1}

On moving towards the lower wavenumber region, the weak absorption peaks located at 1633 cm^{-1} (CdS-St) and 1639 cm^{-1} (CdS-Gl) were found which could be attributed to C=O stretching of carbonyl functional groups present in starch or glucose or adsorbed atmospheric carbon dioxide in CdS [33-35]. On moving further towards the lower wavenumber region; the peaks at 1361 cm^{-1} (CdS-St) and 1356 cm^{-1} (CdS-Gl) were recorded, representing the anti-symmetric bending of $-\text{CH}_3$ corresponding to starch or glucose [36,37]. The C-O and S-O stretching vibration of starch/glucose or sulphate respectively give its broad and weak peaks at 1095 cm^{-1} (CdS-St) and 1005 cm^{-1} (CdS-Gl) [38]. These observations convincingly support the template role of starch/glucose which prevents the agglomeration of CdSNPs. Moreover, a peak near $500\text{-}550 \text{ cm}^{-1}$ suggested the metal-Sulphur (M-S) bond, indicating the synthesis of CdSNPs [39-41]. The small and weak absorptions at 549 cm^{-1} (CdS-St) and 517 cm^{-1} (CdS-Gl) are associated with the characteristic peak of CdSNPs which correspond

to the findings observed by P. S. Khewet al. [42], X. Lu et al. [43], X. Lu et al. [44], T. P. Martin et al. [45] and Z. Qiao et al. [46]. Hence the presence of major functional groups of starch and glucose-capped CdSNPs was assessed by FTIR analysis. The data of FTIR analysis are tabulated in table 1.

3.2 Optical properties

The UV-visible spectrum of starch-capped and glucose-capped CdSNPs (CdS-St and CdS-Gl) is shown in figure 2.

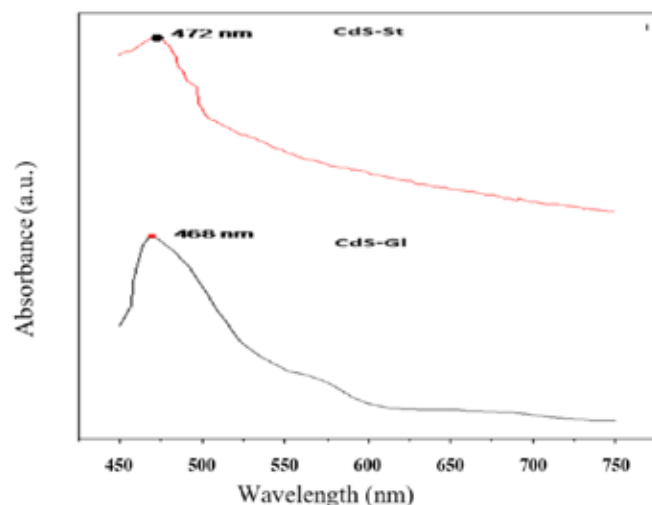


Figure 2. UV-visible spectra of starch and glucose-capped CdSNPs (CdS-St and CdS-Gl)

The spectrum depicts a well-defined, blue-shifted absorption peak. The spectrum shows a well-defined absorption peak at 472 nm (2.63 eV) for CdS-St and 468 nm (2.65 eV) for CdS-Gl. It was observed that the binding energy of the exciton of CdS-St and CdS-Gl was slightly increased as compared to bulk CdS, which shows absorbance at 512 nm (2.42 eV) as suggested by S. Muruganandam et al. [47]. This is attributed to the higher binding energy of the electron-hole pair

Table 1. FTIR peaks of FTIR spectra of starch and glucose-capped CdSNPs (CdS-St and CdS-Gl).

Absorption (cm^{-1})		Functional Group	Intensity of Peak	Remarks and References
CdS-St	CdS-Gl			
3280	3265	O-H stretching	Strong, Broad	Starch, Glucose or Water [33, 34]
1633	1639	C=O stretching	Strong	Starch, Glucose [33-35]
1361	1356	-CH bending of CH_3	Weak	Starch, Glucose [36, 37]
1095	1005	C-O stretching	Small	Starch or Glucose [38]
549	517	Cd-S stretching	Small, weak	CdSNPs [39-46]

by correlating with the report of M. Maleki et al. [48], suggesting the synthesis of CdSNPs. The quantum confinement of photo-generated electron-hole pair is associated with the nanometer scale particle size [49]. In this way, the formation of CdSNPs was confirmed by UV-visible spectroscopy and this result agrees with the FTIR results explaining the presence of spectra associated with the synthesized CdSNPs.

3.3 Morphological characterization

X-ray diffraction (XRD) result of powdered starch and glucose-capped CdSNPs (CdS-St and CdS-Gl) is shown in figure 3.

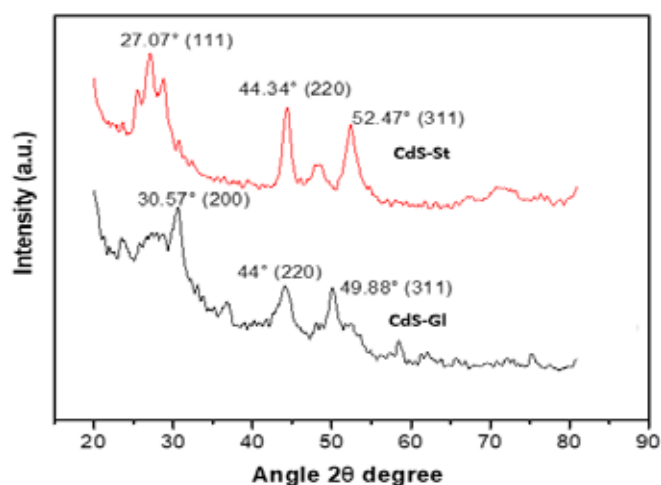


Figure 3. X-ray diffraction graph of starch and glucose capped CdSNPs (CdS-St and CdS-Gl) in the region of 2θ degree of 20° - 80°

The diffraction peaks for CdS-St were obtained at 2θ values of 27.57° , 44.34° and 52.47° corresponding to (111), (220) and (311) miller reflection planes while the diffraction peaks for CdS-Gl were obtained at 2θ values of 30.57° , 44.00° and 49.88° corresponding to (200), (220) and (311) miller reflection planes respectively [50-52]. These outcomes comply with the peaks of pure CdS crystals, corresponding to the JCPDS file number 10-454 [53]. It is quite interesting to note that all the investigated samples have quite similar XRD patterns confirming the presence of the cubic (Zinc blende phase) structure, in agreement with Marin Jet al. [54] and Birajdar et al. [55]. The average crystallite size was calculated with the help of Scherrer's equation using the diffraction intensity of the peak that has the highest intensity [32]. The average crystallite

size of CdSNPs was determined to be 11.48 nm and 16.03 nm for CdS-St and CdS-Gl, respectively. It revealed that CdS-Gl were agglomerated to a greater extent as compared to CdS-St. However, both capping agents restrict the particle size in the nanometer range, showing promising results in stabilized CdSNPs synthesis [56]. These findings are summarized in Table 2. Moreover, the diffraction peaks are broadened as compared to bulk CdS due to the reduced crystallite size, extensive surface defects and powdered form of CdSNPs, as reported previously by R. Banerjee et al. [57] and H. L. Lee et al. [58]. XRD analysis, accordingly, correlates with the results of UV-visible and FTIR spectroscopy which support the synthesis of CdSNPs.

Table 2. Crystallite phase and average crystallite size obtained from X-ray diffraction data.

NPs	2θ (degree)	hkl	Crystallite phase	Average crystallite size (nm)
CdS-St	25.57	111	Cubic	11.48[50-55]
	44.34	220		
	52.41	311		
CdS-Gl	30.57	200	Cubic	16.03[50-55]
	44.00	220		
	52.47	311		

3.4 Antimicrobial activities

3.4a. Antibacterial activities

A comparison of positive and negative controls of the inhibition zone of CdS-St and CdS-Gl is presented in figure 4. The antimicrobial activities of the synthesized CdSNPs (CdS-St and CdS-Gl) were studied by agar well diffusion assay against four bacterial species. Two species; *S. typhi* and *S. aureus* were found to be inhibited by the NPs while the rest of the bacteria were resistant. Therefore, active transport, enzymatic action and formation of nucleic acids are arrested in the periplasmic space, causing apoptosis [60]. The inhibitions by the CdSNPs were observed to be lesser than the positive control which is summarized in table 3.

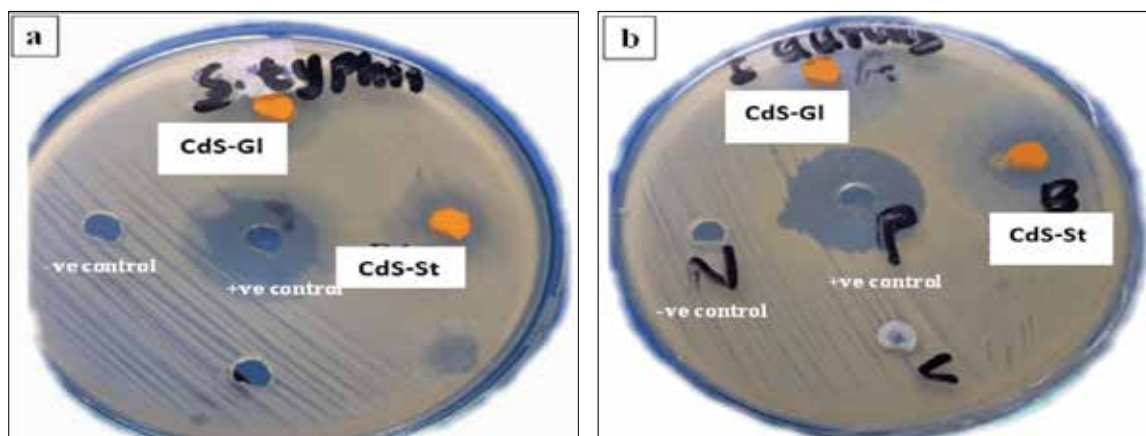


Figure 4. Photographs showing antimicrobial tests of CdSNPs against (a) *S. typhi* and (b) *S. aureus*

Table 3. Summary of the antibacterial properties shown by CdSNPs against *S. typhi* and *S. aureus*, methods used as per literature works [59-60].

Name of bacteria	CdSNPs	Size of the zone of inhibition (mm)		
		NPs	+ve control	-ve control
<i>S. typhi</i>	CdS-St	15 mm	25 mm	-
	CdS-GI	10 mm	25 mm	-
<i>S. aureus</i>	CdS-St	8 mm	26 mm	-
	CdS-GI	8 mm	26 mm	-

3.4b. Antifungal activities

The zone of inhibition of CdSNPs compared to the positive and negative controls is presented in figure 5. The antifungal activity of two synthesized CdSNPs, CdS-St and CdS-GI were studied by well diffusion method against four fungal strains. Among them, only the fungal strain *A. flavus* was found to be inhibited by the CdSNPs, whereas the rest of the fungi were found to be resistant. The inhibitions by the CdSNPs were observed to be lesser than the positive control which is summarized in Table 4. As compared to antibacterial activity, the mechanism of antifungal activity by the CdSNPs is quite different. The fungal strains produce an excess of nucleic acid through the stress response of fungal hyphae against the CdSNPs leading to cell death [27, 28].

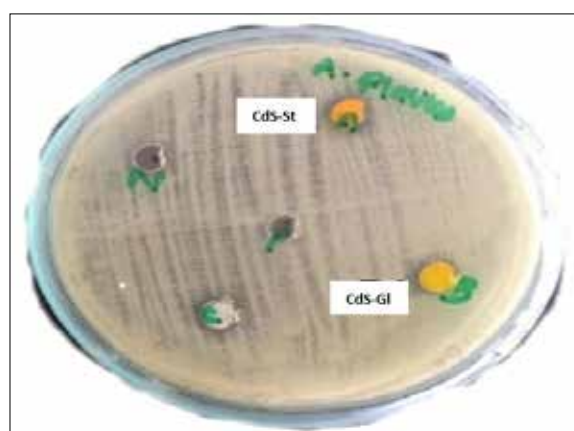


Figure 5. Photographs showing an antifungal test of CdSNPs against *A. flavus*

Table 4. Antifungal properties shown by CdSNPs against *A. flavus* [23].

CdSNPs	Zone of Inhibition		
	NPs	+ve control	-ve control
CdS-St	6 mm	15 mm	-
CdS-GI	6 mm	15 mm	-

4. Conclusions

This research work is encircled in an easy, inexpensive, and environmentally friendly way for the synthesis of carbohydrate-capped CdSNPs. The work was completed under the chemical precipitation method for the synthetic procedure. The following conclusions have been drawn:

- A new synthetic route of CdSNPs was applied.
- In FTIR analysis, the peak in the 500-550 cm^{-1} absorption region confirmed the characteristic peak associated with CdSNPs. Moreover, it contains the peaks associated with the

functional groups of starch and glucose which suggested that the particles were well capped by capping agents.

- UV-visible spectroscopy showed a well-recognized, blue-shifted absorption peak at 472 nm and 468 nm for starch and glucose-capped CdSNPs, respectively.
- XRD plots showed the crystal structure in the nanometer scale range. The average crystallite size of CdSNPs was determined to

be 11.48 nm and 16.03 nm for starch-capped and glucose-capped CdSNPs, respectively. The XRD pattern also suggested the crystal structure of the lattice was in cubic phase which was marked by (111), (200), (220) and (311) miller indices of the lattice.

- CdSNPs were found to be highly effective for two bacterial strains *S. typhi* and *S. aureus* and a fungal strain *A. flavus*.

Acknowledgements

The authors express their sincere thanks to Mr. Komal Prasad Malla and Ms. Prasamsha Panta for their support, suggestions, and encouragement during the experiment. The authors further acknowledge Prof. Dr. Meena Rajbhandari for UV-Vis spectroscopy, Assoc. Prof. Dr. Sabita Shrestha for FTIR spectroscopy, Dr. Suresh Kumar Dhungel (Nepal Academy of Science and Technology) for X-ray diffraction studies, Ms. Bhagwati Gaire and Ms. Sami Poudel for antimicrobial analyses.

References

- [1] A. Rastar, M. E. Yazdanshenas, A. Rashidi, S. M. Bidoki, Theoretical Review of Optical Properties of Nanoparticles, *Journal of Engineered Fibers Fabrics*, 2013, 8, 85-96. <http://doi.org/10.1177/155892501300800211>.
- [2] A. B. Asha, R. Narain, *Polymer Science and Nanotechnology Elsevier* 2020, pp. 343-59.
- [3] L. Wang, C. Hu, L. Shao, The Antimicrobial Activity of Nanoparticles: Present Situation and Prospects for the Future, *International Journal of Nanomedicine*, 2017, 12, 1227-1249. <https://doi.org/10.2147/IJN.S121956>.
- [4] C. C. Yang, Y. W. Mai, *Materials Science and Engineering R: Reports*, 2014, 79, 1-14. <http://dx.doi.org/10.1016%2Fj.mser.2014.02.001>.
- [5] G. Wang, *Nanotechnology: The New Features*, 2018, <https://arxiv.org/abs/1812.04939>. (Accessed 8 May 2022).
- [6] N. A. Mir, A. Khan, K. Umar, M. Muneer, Photocatalytic Study of a Xanthene Dye Derivative, Phloxine B in Aqueous Suspension of TiO₂: Adsorption Isotherm and Decolourization Kinetics, *Energy and Environmental Focus*, 2013, 2, 208-216. <https://doi.org/10.1166/eef.2013.1052>.
- [7] M. A. Khan, A. Ahmad, K. Umar, S. A. Nabi, Synthesis, Characterization and Biological Applications of Nanocomposites for the Removal of Heavy Metals and Dyes, *Industrial and Engineering Chemistry Research*, 2015, 54, 76-82. <https://doi.org/10.1021/ie504148k>.
- [8] S. Sultana, M. Z. Khan, K. Umar, A. S. Ahmed, M. Shahadat, SnO₂-SrO Based Nanocomposites and Their Photocatalytic Activity for the Treatment of Organic Pollutants, *Journal of Molecular Structure*, 2015, 1098, 393-399. <https://doi.org/10.1016/j.molstruc.2015.06.032>.
- [9] Z. A. Peng, X. Peng, Formation of High-Quality CdTe, CdSe, and CdS Nanocrystals Using CdO as Precursor, *Journal of American Chemical Society*, 2001, 123, 183-184. <https://doi.org/10.1021/ja003633m>.
- [10] A. Salem, E. Saion, N. M. Al-Hada, H. K. Mohamed, A. H. Shaari, C. A. C. Abdullah, S. Radiman, Thermal Calcination-Based Production of SnO₂ Nanopowder: An Analysis of SnO₂ Nanoparticle Characteristics and Antibacterial Activities, *Results in Physics*, 2017, 7, 1556-1562. <http://dx.doi.org/10.3390/nano8040250>.
- [11] A. Mercy, R. S. Selvaraj, B. M. Boaz, A. Anandhi, R. Kanagadurai, Synthesis, Structure and Optical Characterization of Cadmium Sulphide Nanoparticles, *Indian Journal of Pure & Applied Physics*, 2013, 51, 448-452. [http://nopr.niscair.res.in/bitstream/123456789/18353/1/IJPAP%2051\(6\)%20448-452.pdf](http://nopr.niscair.res.in/bitstream/123456789/18353/1/IJPAP%2051(6)%20448-452.pdf). (Accessed 8 May 2022).

- [12] R. Banerjee, R. Jayakrishnan, P. Ayyub, Effect of the Size-Induced Structural Transformation on the Band Gap in CdS Nanoparticles, *Journal of Physics: Condensed Matter*, 2005, 12(50). <https://doi.org/10.1088/0953-8984/12/50/325>.
- [13] A. F. G. Monte, N. O. Dantas, P. C. Morais, D. Rabelo, Synthesis and Characterization of CdS Nanoparticles in Mesoporous Copolymer Template, *Brazilian Journal of Physics*, 2006, 36, 427-429. <https://doi.org/10.1590/S0103-97332006000300052>.
- [14] C. Tyagi, A. Sharma, R. Kurchania, Synthesis of CdS Quantum Dots Using Wet Chemical Co-precipitation Method, *Journal of Non-Oxide Glasses*, 2014, 6, 23-26. <https://doi.org/d292/ae3c970db627d8da58430a0af58169615e75>.
- [15] C. A. Fernandez, C. M. Wai, Continuous Tuning of Cadmium Sulfide and Zinc Sulfide Nanoparticle Size in a Water-in-Supercritical Carbon dioxide Microemulsion, *Chemistry of European Journal*, 2007, 13, 5838-5844. <https://doi.org/10.1002/chem.200601259>.
- [16] G. Z. Wang, W. Chen, C. H. Liang, Y. W. Wang, G. W. Meng, L. D. Zhang, Preparation and Characterization of CdS Nanoparticles by Ultrasonic Irradiation, *Inorganic Chemistry Communications*, 2001, 4, 208-210. [https://doi.org/10.1016/s1387-7003\(01\)00172-1](https://doi.org/10.1016/s1387-7003(01)00172-1).
- [17] Y. Lu, L. Li, Y. Din, F. Zhang, Y. Wang, W. Yu, Hydrothermal synthesis of functionalized CdS nanoparticles and their application as fluorescence probe in the determination of uracil and thymine, *Journal of Luminescence*, 2011, 132(244-249). <https://pdfs.semanticscholar.org/e5a6/f90f795b4588017e224662b2972a2493281d.pdf> (Accessed 8 May 2020).
- [18] S. A. E. Soheir, H. T. Rania, M. T. Amany, O. A. E. Mohamed, A. M. Hanady, Antimicrobial Activity of Bio and Chemical Synthesized Cadmium Sulfide Nanoparticles, *The Egyptian Journal of Hospital Medicine*, 2014, 70, 1494-1507. <https://platform.almanhal.com/Reader/Article/113858>.
- [19] A. B. Saraswathi, R. Kilaparti, P. Manjunatha, Comparison of Various Organic Stabilizers as Capping Agents for CdS Nanoparticles Synthesis, *Journal of Materials Science: Materials in Electronics*, 2007, 18, 1109-1113. <https://doi.org/10.1007/s10854-007-9139-2>.
- [20] V. Singh, P. K. Sharma, P. Chauhan, Synthesis of CdS Nanoparticles with Enhanced Optical Properties, *Materials Characterization*, 2011, 62(1), 43-52. <https://doi.org/10.1016/j.matchar.2010.10.009>.
- [1] K. T. Yong, Y. Wang, I. Roy, H. Rui, M. T. Swihart, W. C. Law, S. K. Kwak, J. Liu, S. D. Mahajan, J. L. Reynolds, Preparation of Quantum Dot/Drug Nanoparticle Formulations for Traceable Targeted Delivery and Therapy, *Theranostics*, 2012, 2(7), 681-694. <https://doi.org/10.7150/thno.3692>.
- [21] J. S. Kim, E. Kuk, K. N. Yu, J. H. Kim, S. J. Park, H. J. Lee, S. H. Kim, Y. K. Park, Y. H. Park, C. Y. Hwang, Y. K. Kim, Y. S. Lee, D. H. Jeong, M. H. Cho, Antimicrobial Effects of Silver Nanoparticles, *Nanomedicine: Nanotechnology, Biology and Medicine*, 2007, 3(95-101). <https://doi.org/10.1016/j.nano.2006.12.001>.
- [22] S. Rajeshkumar, M. Ponnaniakamideen, C. Malarkodi, M. Malini, G. Annadurai, Microbe-mediated Synthesis of Antimicrobial Semiconductor Nanoparticles by Marine Bacteria, *Journal of Nanostructure in Chemistry*, 2014, 4: 96. <https://doi.org/10.1007/s40097-014-0096-z>.
- [23] C. Malarkodi, S. Rajeshkumar, K. Paulkumar, M. Vanaja, G. Gnanajobitha, G. Annadurai, Biosynthesis and Antimicrobial Activity of Semiconductor Nanoparticles against Oral Pathogens, *Bioinorganic Chemistry and Applications*, Article ID 347167, 2014, 1-10. <https://doi.org/10.1155/2014/347167>.
- [24] Z. M. Xiu, Q. B. Zhang, H. L. Puppala, V. L. Colvin, P. J. J. Alvarez, Negligible Particle-Specific Antibacterial Activity of Silver Nanoparticles, *Nano Letters*, 2012, 12(8), 4271-4275. <https://doi.org/10.1021/nl301934w>.
- [25] D. Mubarak Ali, N. Thajuddin, K. Jegannathan, M. Gunasekaran, Plant Extract Mediated Synthesis of Silver and Gold Nanoparticles and its Antibacterial Activity Against Clinically Isolated Pathogens, *Colloids Surface B: Biointerfaces*, 2011, 85(2), 360-365. <https://doi.org/10.1016/j.colsurfb.2011.03.009>.
- [26] L. He, Y. Liu, A. Mustapha, M. Lin, Antifungal Activity of Zinc Oxide Nanoparticles Against *Botrytis cinerea* and *Penicillium expansum*, *Microbiological Research*, 2011, 166(3), 207-215. <https://doi.org/10.1016/j.micres.2010.03.003>.

- [27] N. H. Patel, M. P. Deshpande, S. H. Chaki, H. R. Keharia, Tuning of Optical, Thermal and Antimicrobial Capabilities of CdS Nanoparticles with Incorporated Mn Prepared by Chemical Method, *Journal of Materials Science: Materials in Electronics*, 2017, <https://doi.org/10.1007/s10854-017-6865-y>.
- [28] A. Shivashankarappa, K. R. Sanjay, Escherichia coli- Based Synthesis of Cadmium Sulfide Nanoparticles, Characterization, Antimicrobial and Cytotoxicity Studies, *Brazilian Journal of Microbiology*, 2020, 51, 939-948. <https://dx.doi.org/10.1007/s42770-020-00238-9>.
- [29] A. R. RasuChettiar, L. Marasamy, S. Velumani, G. Oza, Synthesis and Characterization of Cadmium Sulphide Nanoparticles by Chemical Precipitation Method, *Journal of Nanoscience and Nanotechnology*, 2015, 15(11), 8434-8439. <https://doi.org/10.1166/jnn.2015.11472>.
- [30] P. Vithu, S. K. Dash, K. Rayaguru, M. K. Panda, M. Nedunchezhiyan, 2020 Optimization of Starch Isolation Process for Sweet Potato and Characterization of the Prepared Starch, *Journal of Food Measurement and Characterization*, 2020, 14, 1520-1532. <https://doi.org/10.1007/s11694-020-00401-8>.
- [31] H. P. Klug, L. E. Alexander, Determination of Crystalline Size with the X-Ray Spectrometer, *Journal of Applied Physics*, 1950, 21(137). <https://doi.org/10.1063/1.1699612>.
- [32] N. Santha, K. G. Sudha, K. P. Vijayakumari, V. U. Nayar, S. N. Moorthy, Raman and Infrared Spectra of Starch Samples of Sweet Potato and Cassava, *Proceedings of the Indian Academy of Sciences (Chemical Sciences)*, 1990, 102, 705-712. <https://www.ias.ac.in/article/fulltext/jcsc/102/05/0705-0712>.
- [33] B. Shujahadeen, A. Mariwan, R. Salah, Gh. Omed, Synthesis and Characterization of CdS Nanoparticles Grown in a Polymer Solution using in-situ Chemical Reduction Technique, *Synthesis and Characterization of CdS Nanoparticles Grown in a Polymer Solution using in-situ Chemical Reduction Technique*, *International Journal of Electrochemical Science*, 2007, 12, 3263-3274. <https://doi.org/10.20964/2017.04.10>.
- [34] B. C. Smith, *The Carbonyl Group, Part I: Introduction, Spectroscopy*, 2017, 32(9), 31-36. <https://www.spectroscopyonline.com/view/carbonyl-group-part-i-introduction>. (Accessed 8 May 2022).
- [35] J. J. Cael, J. L. Koenig, J. Blackwell, *Infrared and Raman Spectroscopy of carbohydrates, Part VI: Normal coordinate analysis of V-amylose*, *Biopolymers*, 1975, 14, 1885-1903. <https://doi.org/10.1002/bip.1975.360140909>.
- [36] Z. P. Zhang, M. Z. Rong, M. Q. Zhang, C. Yuan, Alkoxyamine with Reduced Homolysis Temperature and its Application in Repeated Autonomous Self-healing of Stiff Polymer, *Polymer Chemistry*, 2013, 4, 4648-4654. <https://doi.org/10.1039/C3PY00679D>.
- [37] N. Ramamurthy, S. Kannan, Fourier Transform Infrared Spectroscopic Analysis of a Plant (*Calotropis gigantea* Linn) from an Industrial Village, Cuddalore Dt., Tamilnadu, *Indian Romanian Journal of Biophysics*, 2007, 17(4). <https://www.rjb.ro/articles/192/art%2006%20Ramamurthy%20doc.pdf>. (Accessed 8 May 2022).
- [38] G. Socrates, *Infrared Characteristic Group Frequencies*, John Wiley & Sons, 1980, ISBN 13: 9780471275923.
- [39] G. Socrates, *Infrared and Raman Characteristic Group Frequencies: Tables and Charts*, Wiley Chichester, 2001, ISBN: 0471852988.
- [40] K. Nakamoto, *Infrared and Raman Spectra of Inorganic and Coordination Compounds*, Wiley Online Library, 1978. <https://doi.org/10.1002/0470027320.s4104>.
- [41] P. S. Khiew, N. M. Huang, S. Radiman, M. S. Ahmad, Synthesis and Characterization of Conducting Polyaniline-Coated Cadmium Sulfide Nanocomposites in Reverse Microemulsion, *Materials Letters*, 2004, 58, 516- 521. [https://doi.org/10.1016/s0167-577x\(03\)00537-8](https://doi.org/10.1016/s0167-577x(03)00537-8).
- [42] X. Lu, Y. Yu, L. Chen, H. Mao, W. Zhang, Y. Wei, Preparation and Characterization of Polyaniline Microwires Containing CdS Nanoparticles, *Chemical Communications*, 2004, 1522-1523. <https://doi.org/10.1039/B403105A>.
- [43] X. Lu, H. Gao, J. Chen, D. Chao, W. Zhang, Y. Wei, Poly (Acrylic Acid)-Guided Synthesis of Helical Polyaniline/CdS Composite Microwires, *Nanotechnology*, 2005, 16, 113-117. <https://doi.org/10.1088/0957-4484/16/1/023>.
- [44] T. P. Martin, H. Schaber, *Spectrochimica Acta*, 1982, 38(6), 655-660. [https://doi.org/10.1016/0584-8539\(82\)80086-X](https://doi.org/10.1016/0584-8539(82)80086-X).

- [45] Z. Qiao, Y. Xie, G. Li, Y. Zhu, Y. Qian, Journal of Materials Chemistry, 2009, 19, 869-884. <https://doi.org/10.1039/B816463K>.
- [46] S. Muruganandam, G. Anbalagan, G. Murugadoss, Optical, Electrochemical and Thermal Properties of Co²⁺-Doped CdS Nanoparticles Using Polyvinylpyrrolidone, Applied Nanoscience, 2015, 5, 245-253. <https://doi.org/10.1007/s13204-014-0313-6>.
- [47] M. Maleki, M. G. Sasani, S. Mirdamadi, R. Ghasemzadeh, A Facile Route for Preparation of CdS Nanoparticles, Semiconductor Physics, Quantum Electronics and Optoelectronics, 2007, 10, 30-32. <https://doi.org/10.15407/spqe01.01.030>.
- [48] L. Yao, G. Xu, X. Yang, Y. Luan, CdS@SiO₂ Nanoparticles Synthesized from Polyoxyethylene (10) Tertoctylphenyl Ether Based Reverse Microemulsion, Colloids and Surface A: 333:1, 2009. <https://doi.org/10.1016/j.colsurfa.2008.09.019>.
- [49] S. Muruganandam, G. Anbalagan, G. Murugadoss, Synthesis, Structural, Optical and Thermal Properties of CdS:Zn²⁺ Nanoparticles, Applied Nanoscience, 2014, 4, 1013–1019. <https://doi.org/10.1007/s13204-013-0284-z>.
- [50] L. Ding, T. Li, Y. Zhong, C. Fan, J. Huang, Synthesis and Characterization of a Novel Nitric Oxide Fluorescent Probe CdS-PMMA Nanocomposite via In-Situ Bulk Polymerization, Materials Science and Engineering: C, 2014, 35, 29–35. <https://doi.org/10.1016/j.msec.2013.10.012>.
- [51] J. Yang, J. Yu, J. Fan, D. Sun, W. Tang, X. Yang, Journal of Hazardous Materials, 2011, 189, 377–383. <https://doi.org/10.1016/j.jhazmat.2011.02.048>.
- [52] S. Muruganandam, G. Anbalagan, G. Murugadoss, Biotemplated Preparation of CdS Nanoparticles/Bacterial Cellulose Hybrid Nanofibres for Photocatalysis Application, Applied Nanoscience, 2011, 4, 1013–1019. <https://doi.org/10.1016/j.jhazmat.2011.02.048>.
- [53] J. Marin, C. G. Castanedo, G. Delgado, M. A. Frutis, R. Perez, O. Angel, Very Sharp Zinc Blende-Wurtzite Phase Transition of CdS Nanoparticles, Superlattices and Microstructures, 2017, 102, 442-450. <https://doi.org/10.1016/j.spmi.2017.01.007>.
- [54] S. D. Birajdar, P. Khirade, A. V. Humbe, K. M. Jadhav, Crystallographic and Optical Properties of CdS Nanoparticles Synthesized by Wet Chemical Route, International Journal of Academic Research in Business, Arts and Science (IJARBAS), 2014, Vol. 1(1). ISSN: 2394-4072.
- [55] B. Ajitha, Y. A. Kumar Reddy, P. S. Reddy, H. J. Jeon, C. W. Ahn, Role of Capping Agents in Controlling Silver Nanoparticles Size, Antibacterial Activity and Potential Applications as Optical Hydrogen Peroxide Sensors, The Royal Society of Chemistry (RSC) Advances, 2016, 6, 36171–36179. <https://doi.org/10.1039/C6RA03766F>.
- [56] R. Banerjee, R. Jayakrishnan, P. Ayyub, Effect of the Size-Induced Structural Transformation on the Band Gap in CdS Nanoparticles, Journal of Physics: Condensation Matter, 2000, 12, 10647-10654. <https://doi.org/10.1088/0953-8984/12/50/325>.
- [57] H. L. Lee, A. M. Issam, M. Belmahi, M. B. Assouar, H. Rinnert, M. Alnot, Synthesis and Characterizations of Bare CdS Nanocrystals Using Chemical Precipitation Method for Photoluminescence Application, Journal of Nanomaterials, 2009, Article ID 914501, 1-9. <https://doi.org/10.1155/2009/914501>.
- [58] M. Shukla, S. Kumari, S. Shukla, R. K. Shukla, Potent Antimicrobial Activity of Nano CdO Synthesized Via Microemulsion Scheme, Journal of Materials and Environmental Science, 2012, 3(4), 678-685. https://www.jmaterenvironsci.com/Document/vol3/vol3_N4/68-JMES-148-2011-Shukla.pdf. (Accessed on 8 May 2022).
- [59] S. Zarchi, A. Javed, M. J. Ghani, S. Soufian, F. B. Firouzabadi, A. B. Moghadden, S. H. Mirjilili, Comparative Study of Antimicrobial Activities of TiO₂ and CdO Nanoparticles Against the Pathogenic Strain of Escherichia coli, Iranian Journal Pathology, 2010, 5(2), 83-89. https://ijp.iranpath.org/article_8830_715048794d0fbd1a50562cfc002effcc.pdf. (Accessed on 8 May 2022).